

Mechanical and Energy Engineering

Numerical Investigation of Aerodynamic Characteristics of Supercritical RAE2822 Airfoil with Gurney Flap

Iman Jabbar Ooda

Lecturer

Department of Aeronautical Eng.,
University of Baghdad,
Baghdad-Iraq

Iman.Jabbar@coeng.uobaghdad.edu.iq

ABSTRACT

Gurney flap (GF) is well-known as one of the most attractive plain flaps because of the simple configuration and effectiveness in improving the lift of the airfoil. Many studies were conducted, but the effects of GF on the various airfoil types need to be further investigated. This study aimed to clarify the effect of GF in the case of the supercritical airfoil RAE2822. This research includes a steady, two-dimensional computational investigation carried out on the supercritical airfoil type RAE-2822 to analyze Gurney flap (GF) effects on the aerodynamic characteristics of this type of airfoil utilizing the Spalart-Allmaras turbulence model within the commercial software Fluent. The airfoil with the Gurney flap was analyzed for three different height values 1%c, 2%c, and 3%c, and five mounting angles (30°, 45°, 60°, 75°, and 90°) with the axial chord for angles of attack (-1°, -2°, -3°, 0°, 1°, 2°, 3°). The calculations showed that when GF height is increased, the maximum suction pressure on the upper surface increases by 25.4%, 36.5%, and 68.83% when the height of the Gurney flap is 1%c, 2%c, and 3%c, respectively, compared with that on the airfoil without GF. The lift coefficient was also increased, and the shock waves moved downward by increasing GF height. As Gurney flap heights increase, the drag coefficient increases gradually for positive angles of attack but for negative angles of attack. The drag coefficient also decreases with increasing the GF heights. As long as the angle of the mounting is between 45° and 90°, the lift coefficient does not differ on a large scale. For mounting angles less than 45°, the lift coefficient drops quite fast. As a result, reducing the Gurney flap's lift enhancement and the drag coefficient increases gradually for positive angles of attack, but for negative angles, it can be noted that the drag coefficient decreases with increasing the mounting angles of GF. The calculated values of the lift and drag coefficients with an attack angle and pressure coefficient compared with the experimental values, and a good agreement was noticed.

Keywords: Supercritical airfoil RAE 2822, Gurney flap, Aerodynamic characteristics, Lift enhancement.

*Corresponding author

Peer review under the responsibility of University of Baghdad.

<https://doi.org/10.31026/j.eng.2022.06.01>

This is an open access article under the CC BY4 license (<http://creativecommons.org/licenses/by/4.0/>).

Article received: 2/1/2022

Article accepted: 23 /2/2022

Article published: 1/6/ 2022

الاستقصاء العددي للخصائص الايروديناميكية لمقطع جناح فوق الحرج نوع مع قلاب كيرني RAE2822

ايمان جبار عودة

مدرس

قسم هندسة الطيران/جامعة بغداد
بغداد/العراق

الخلاصة

يتضمن هذا البحث دراسات حسابية ثنائية الأبعاد للحالة المستقرة والتي تم إجراؤها على الجنيح الفوق الحرج RAE-2822 لتحليل تأثيرات قلاب نوع كيرني على الخصائص الايروديناميكية باستخدام برنامج fluent ونموذج الاضطراب Spalart-Allmaras. تم تحليل مقطع الجناح مع القلاب لثلاث قيم لارتفاع القلاب (1% c, 2% c, 3% c) وخمسة قيم لزوايا تركيب القلاب (30°, 45°, 60°, 75°, 90°) مع الوتر ولزوايا هجوم (3°, 1°, 2°, 0°, 1°, 2°, 3°). تظهر الحسابات انه عند زيادة ارتفاع القلاب سوف يزداد الحد الاقصى لضغط الشفط على السطح العلوي لمقطع الجناح بنسبة (25.4%, 36.5%, 68.83%) عندما يكون ارتفاع القلاب (1% c, 2% c, 3% c) على التوالي مقارنة بمقطع الجناح بدون قلاب. لوحظ زيادة معامل الرفع وتحرك الموجة الصدمية باتجاه الحافة الخلفية لمقطع الجناح مع زيادة ارتفاع القلاب ولكن معامل الكبح يزداد تدريجيا لزوايا هجوم موجبة ولكن يقل بزوايا هجوم سالبة مع زيادة ارتفاع القلاب. طالما ان زوايا تركيب القلاب تتراوح ما بين 45°-90° فان معامل الرفع لايتغير على نطاق واسع وبالنسبة لزوايا تركيب اقل من 45° فان معامل الرفع يقل بسرعة كبيرة مما يقلل من تحسين الرفع للقلاب ومعامل الكبح يزداد تدريجيا لزوايا هجوم موجبة ولكن يقل بزوايا هجوم سالبة مع زيادة زاوية تركيب القلاب. تمت مقارنة القيم المحسوبة لمعاملات الرفع والكبح مع زاوية الهجوم ومعامل الضغط مع القيم التجريبية وتم التوصل إلى توافق جيد.

الكلمات الرئيسية: الجنيح الفوق الحرج، الخواص الايروديناميكية، زيادة معامل الرفع، ارتفاع القلاب.

1. INTRODUCTION

Utilizing high-lift devices to enhance the aerodynamic performance of the airfoils has been an active research area in applied aerodynamics. Flap, a type of high-lift device, is generally used to enhance the aerodynamic performance of the wing sections during flight. Among flap types, as shown in **Fig. 1**, GF is a micro tab that is affixed to the airfoil near the trailing edge on the pressure side. D. Gurney used it on the top trailing edge of the rear wing of the race vehicle he owned to provide additional rearend downforce with minimum aerodynamics disturbances (**Jang, C. S. et al.,1998**). Due to the sharp corner flap, two counter-rotating vortices are formed. The total circulation around the airfoil gets increased, which adds to the lift. For supercritical airfoils, the lift enhancement of the Gurney flap mainly comes from its ability to shift the shock on the upper surface downstream, further delaying the onset of stall.

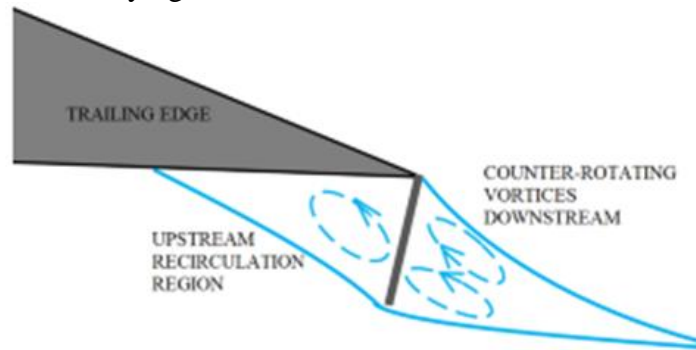


Figure 1. Mean flow field in the presence of Gurney flap (based on (**Liebeck, R. H.,1978**)).



Many researchers studied the effect of the Gurney flap (GF) on the performance of wings (**Mohammed Kheir-aldeen and Ahmed Hamid, 2014**) and experimentally investigated the effects of the GF flap on the aerodynamic properties of the Clark Y-14 airfoil. They have concluded that the serrated Gurney flap significantly increases the lift to drag ratio. Rectangular serrated Gurney flap presents the optimal efficiency amongst serrated GF by improving the ratio of lift to drag up to (42.80%). (**Shubham Jain, et al., 2015**) studied the aerodynamic characteristics of the airfoil 0012 computationally and concluded that the maximum lift improvement with minimum drag could be obtained by using a perpendicular GF to the airfoil's chord with a height of 1.5%*c* and as close to the trailing edge as possible. (**Daniel R. Troolin, et al., 2016**) have investigated the NACA0015 airfoil with and without Gurney flap in a wind tunnel with $Re = 2 \times 10^5$ to examine the wake evolving flow structure via time-resolved PIV and hot-film anemometry frequency measurements. They have noticed a number of the vortex shedding modes associated with attack angle and flap height. (**Xi He, et al., 2016**) investigated the effect of GF on the aerodynamic performance of the SFYT 15 thick airfoil through solving a 2-D steady Reynolds averaged Navier-Stocks (RANS) equations, it has been discovered that increasing airfoil drag with the GF may be a result of increased pressure drag between leeward and windward sides of the actual GF. (**Sanjoy Kumar Saha1, and Md. Mahbulul Alam, 2017**) investigated the effect of serrated Gurney flap on airfoil 2412 computationally and experimentally. This investigation showed that square serration provides the best performance rather than triangular serrated flap and suggested that serrated Gurney flap may lead to reduce the drag in the maximum lift region. (**Nguyen, T. D., et al., 2019**) studied effects of Gurney flap in supercritical airfoil case, SC0414 airfoil through the analysis of lift coefficient in the case of increasing the GF height using Ansys-Fluent software then compared the theoretical results with the experimental result that have been obtained from the testing of the wind tunnel. (**Nguyen, T.D., et al., 2020**) estimated the lift coefficient of SC-0414 airfoil using modified Yamana's method to the flow visualization results obtained by utilizing the smoke tunnel.

In the present work, a steady, two-dimensional computational investigation is carried out on the supercritical airfoil type RAE 2822 for the analysis of Gurney flap (GF) effects on the aerodynamic characteristics of this type of airfoil utilizing the Spalart-Allmaras turbulence model within the commercial software Ansys-Fluent 14.5. Additionally, the lift estimation, wake measurements, and numerical simulations are performed to clarify the low-speed aerodynamic characteristics of the SC airfoil with GF. They observed that when the height of the flap was increased, the lift and drag coefficients increased. Installing a GF with a height equal to 1% of the airfoil chord length significantly improved the low-speed aerodynamic performance.

2. GOVERNING EQUATIONS

The governing equations for computations of a two-dimensional steady turbulent compressible flow, in the absence of gravitational body force, external body force, and any volumetric heat sources, are (**Dhruva Koti and Ayesha Khan M., 2018**).

The continuity equation:

$$\frac{\partial \rho}{\partial t} + \frac{\partial}{\partial x_j} (\rho U_j) = 0 \quad (1)$$

Momentum equation:

$$\frac{\partial}{\partial t} (\rho U_i) + \frac{\partial}{\partial x_j} (\rho U_i U_j) = - \frac{\partial p}{\partial x_i} + \frac{\partial \tau_{ij}}{\partial x_j} \quad (2)$$

And the energy equation:

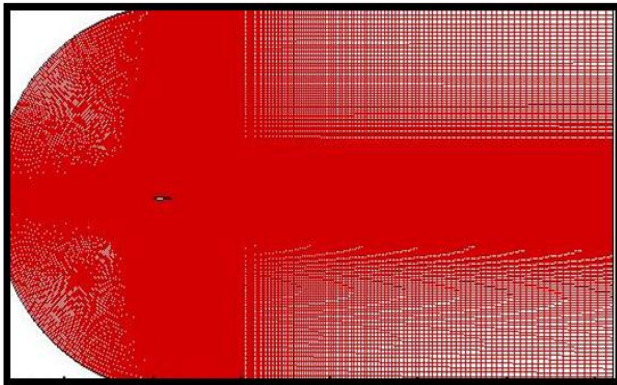
$$\frac{\partial}{\partial t}(\rho h) + \frac{\partial}{\partial x_j}(\rho U_j h) = \frac{\partial p}{\partial t} + U_j \frac{\partial p}{\partial x_j} + \tau_{ij} \frac{\partial U_j}{\partial x_i} - \frac{\partial q_i}{\partial x_i} \quad (3)$$

3. GEOMETRY & GRID GENERATION

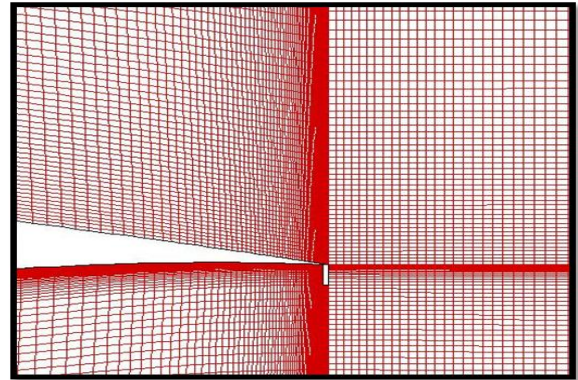
The Ansys-Fluent 14.5 finite element program was used for analyzing the flow around the supercritical RAE2822 airfoil with GF. The airfoil with a chord length of 1m and the GF with a height of 3%c and its mounting angle ($\Phi = 90^\circ$). To create the geometry of an airfoil, the coordinates were taken from (<http://airfoiltools.com/airfoil/naca4digit>). A C-mesh domain was chosen for the flow analysis and generated a structured mesh called 'mapped face mesh'. The dimension of the arc radius is set at 10c, whereas the sides of the other two squares are set at 25c. The airfoil was discretized into 407600 elements with 409377 nodes. The computational domain is shown in **Fig. 2**, and the details of the mesh are shown in **Table 1**.

Table 1. Details of Mesh.

Mesh metric	Min.	Max.	Average	Standard Deviation
Orthogonal quality	1.38016479766344E-02	1	0.974574391848783	0.102652219579658



(a) The distribution of the C-type grid around RAE 2822 airfoil.



(b) Zoom-in view of grids in the vicinity of GF and trailing edge.

Figure 2. Computational domain.

4. VALIDATION STUDY

In order to validate the computational results, pressure coefficient, lift and drag coefficients are compared with the results of experimental work, case 9 of (**AGARD report, 1979**), as shown in **Fig. 3** and **table 2**. The flow conditions of the test case are $M = 0.729$, $AOA = 3.19^\circ$ and $Re = 6.5 \times 10^6$. To compare the computed results with the wind tunnel experimental results, the condition of the flow in the numerical simulation should be corrected to compensate for the wall effects of the wind tunnel. Using the correction method of (**Coakley, T. J., 1987**), Mach number and AOA

are set to be 0.729 and 2.79° , respectively, and $Re = 6.5 \times 10^6$. Good agreement is obtained between the experimental and the present computed results.

Table 2. Comparison of (Cook, P. H., et al., 1979) and the present study.

Report	CL	% error	CD	% error	X _{shock} /c
AGARD report 1979	0.803	-	0.0168	-	0.525
Present work	0.751	6.4%	0.0176	4.5%	0.52

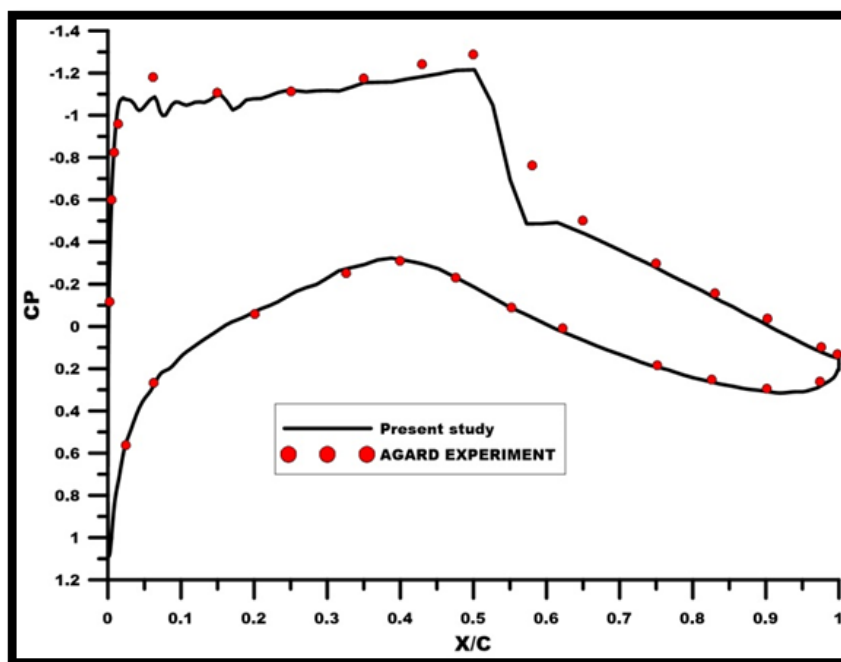


Figure 3. Comparison between computed pressure coefficient and experimental results (Cook, P. H., et al., 1979).

5. RESULTS AND DISCUSSION

The simulations were carried out for the far field Mach number of 0.75 , and the angle of attack varies between -3° to 3° with a 1 -degree increment.

5.1 Pressure coefficient distribution

Pressure coefficient distribution at an $AOA = 0^\circ$ for various Gurney flap (GF) height levels has been illustrated in **Fig.4**. When GF height is $1\%c$, $2\%c$, and $3\%c$, the maximum suction pressure on the airfoil suction surface increased by 25.4% , 36.5% , and 68.83% , respectively, on airfoil without GF. Actually, the GF is a chord alteration: increased camber. In effect, it alters the airfoil Kutta condition. Also, it can be seen that the shock moves downstream with increasing the GF height. The shock delay resulting from the GF may be explained by the increased camber and combined with the rotating vortex at the trailing edge. Vorticities are clearly seen behind the flap

on the trailing edge, as shown in **Fig.5**. It has been believed that a rotating vortex provides “pulling” force to the suction surface, which forces the flow to attach along the surface. Also, flow velocity increases as well by that force. For better illustration in this case, where the Mach number at far-field is 0.75, the Mach number contours are provided in **Fig.6**. **Table 3** shows the effect of GF height on the location of the shock wave.

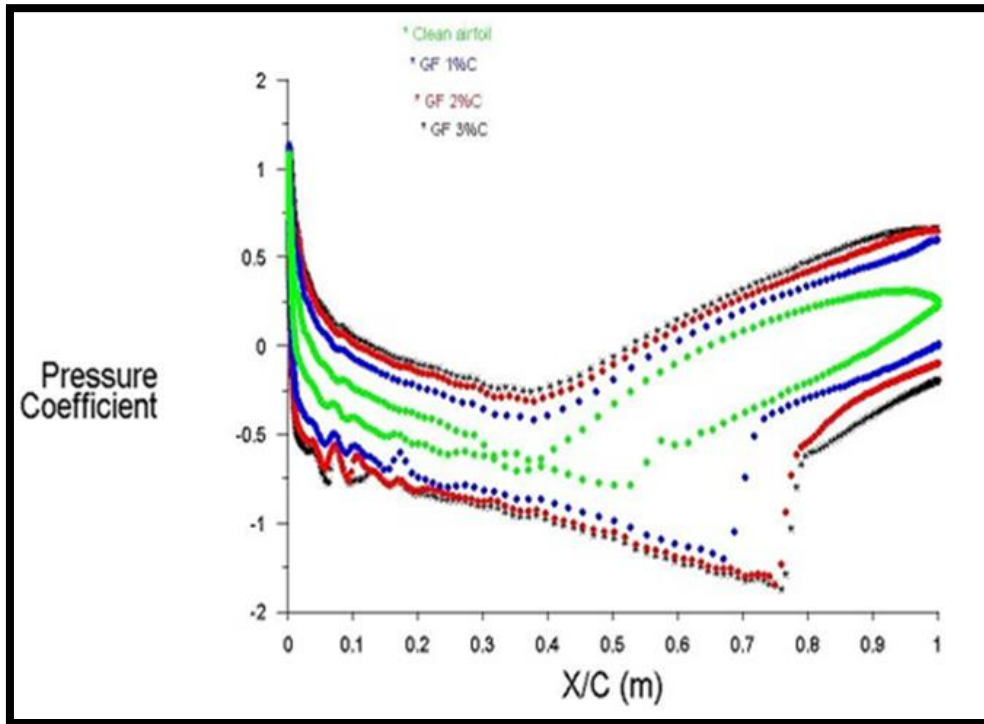
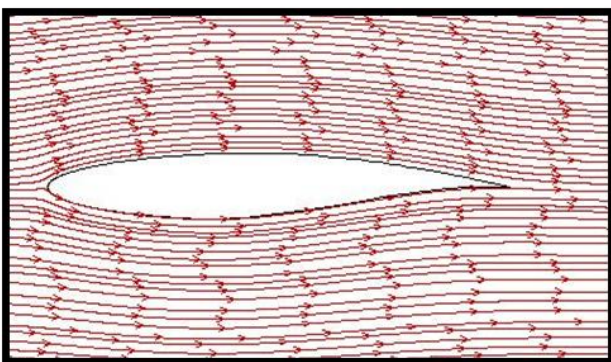
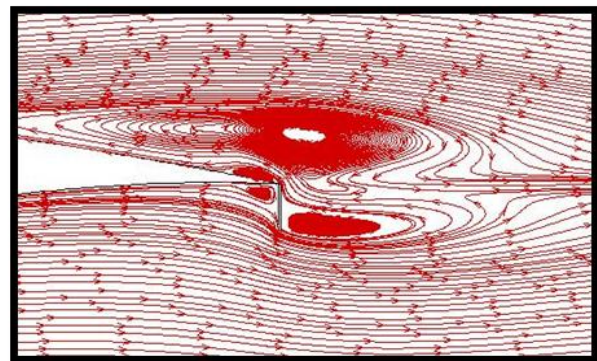


Figure 4. Pressure coefficient distribution for clean airfoil and airfoil with different heights.

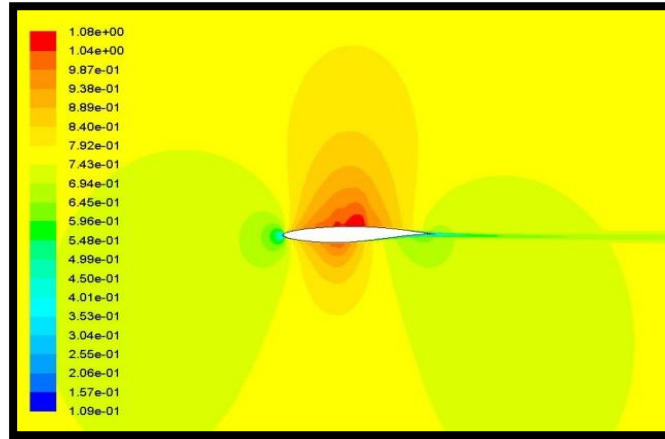


(a)

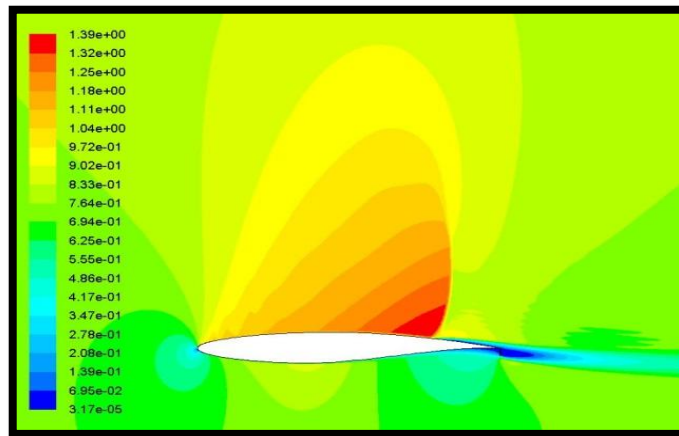


(b)

Figure 5. Streamlines around airfoil without GF (a) and with GF (b).



a) AOA = 0°, clean airfoil



(b) AOA = 0°, with GF

Figure 6. Mach number contour near the airfoil showing the shock on the surface.

Table 3. Effect of GF height on the location of the shock wave.

H(height) of GF	Shock position (x/c)
clean airfoil	0.526
1% c	0.686188
2% c	0.75743
3% c	0.77348

5.2 Lift coefficient

Lift coefficient variation with the AOA for GF height values of 0% (without GF), 1%*c*, 2%*c*, and 3%*c* is depicted in **Fig.7**. Generally, lift coefficient increases with increasing the GF height. The increase in lift coefficient because of changing the GF height from 0%*c* to 1%*c* is greater than the lift coefficient due to changing the height of the GF from 2%*c* to 3%*c*. According to the analyses, the angle of zero lift decreases while the height of the GF increases.

As shown in **Fig.5**, the GF causes the flow to turn downward beyond the flap, indicating the fact that the GF is generating the increase of the lift. This agrees with (Liebeck, R. H.1978) wind tunnel test.

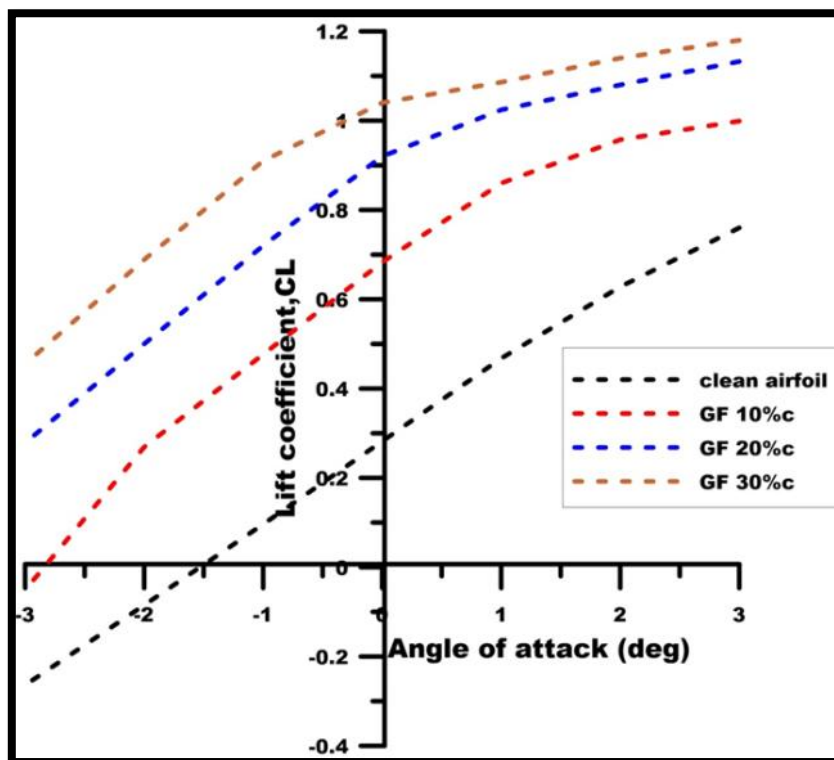


Figure 7. Variation of CL with α for different heights of GF.

5.3 Drag coefficient

Fig.8. depicts the variation of drag coefficient with angles of attack at different GF heights. With the increase in the GF height values, the drag coefficient is gradually increased, the maximum drag coefficient at maximum GF heights of 3% *c* for positive angles of attack, but for negative angles of attack, it can be noted that the drag coefficient decreases with increasing the GF height.

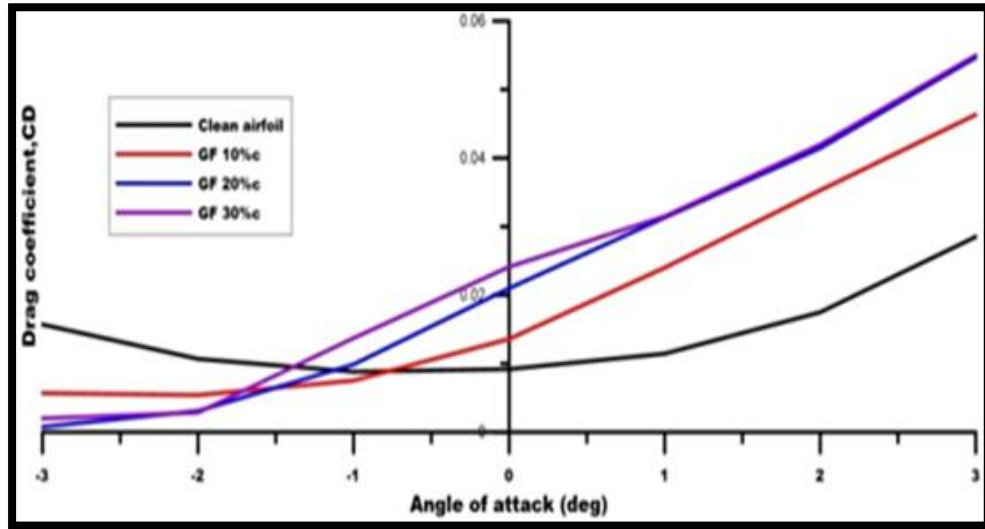


Figure 8. Variation of C_D with α for different heights of GF.

5.4 Effect GF of mounting angle on the aerodynamic characteristics of the airfoil.

5.4.1 Pressure coefficient distribution

The computed pressure coefficient distribution on the airfoil surface with a GF's height of 3% and $AOA = 0^\circ$ is shown in Fig.9. GF Mounting angle only affects the static pressure distribution near the trailing edge. Suction pressure decreases with decreasing the mounting angle, and the location of maximum suction pressure moves downstream with increasing the mounting angle.

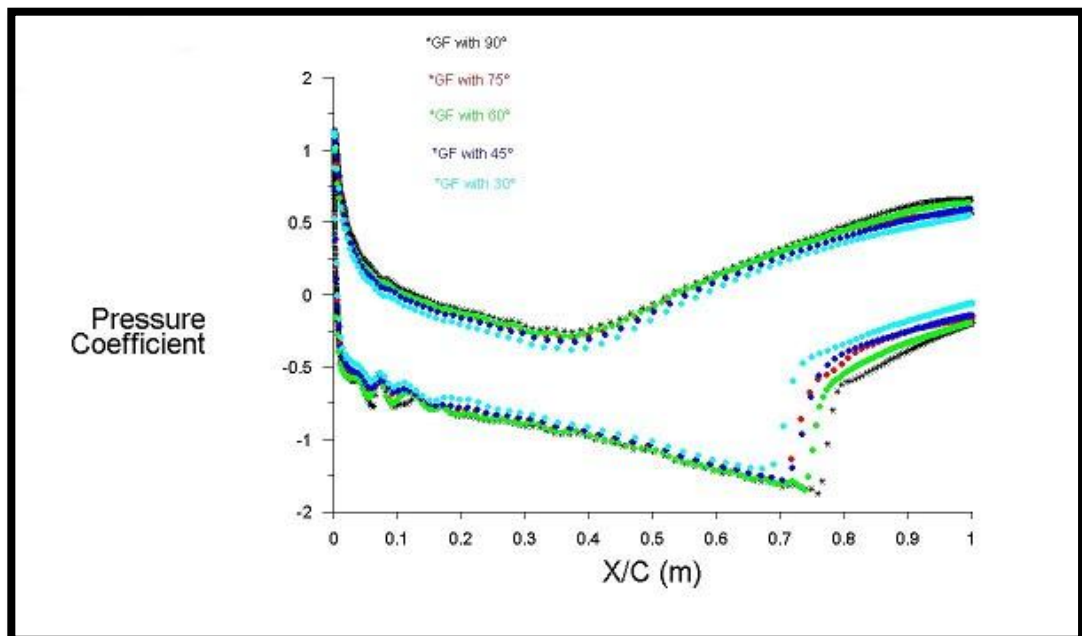


Figure 9. Pressure coefficient distribution for different values of GF's mounting angles at $AOA = 0^\circ$.



5.4.2 Flow streamlines for different values of GF's mounting angles with a height of 3%c and AOA = 0°.

Flow near the trailing edge of the airfoil with GF's height of 3%c and different GF's mounting angles at an AOA of 0° is shown in **Fig.10**. The vortex near the suction surface does not form entirely when the GF's mounting angle drops, resulting in less suction and a decrease in lift.

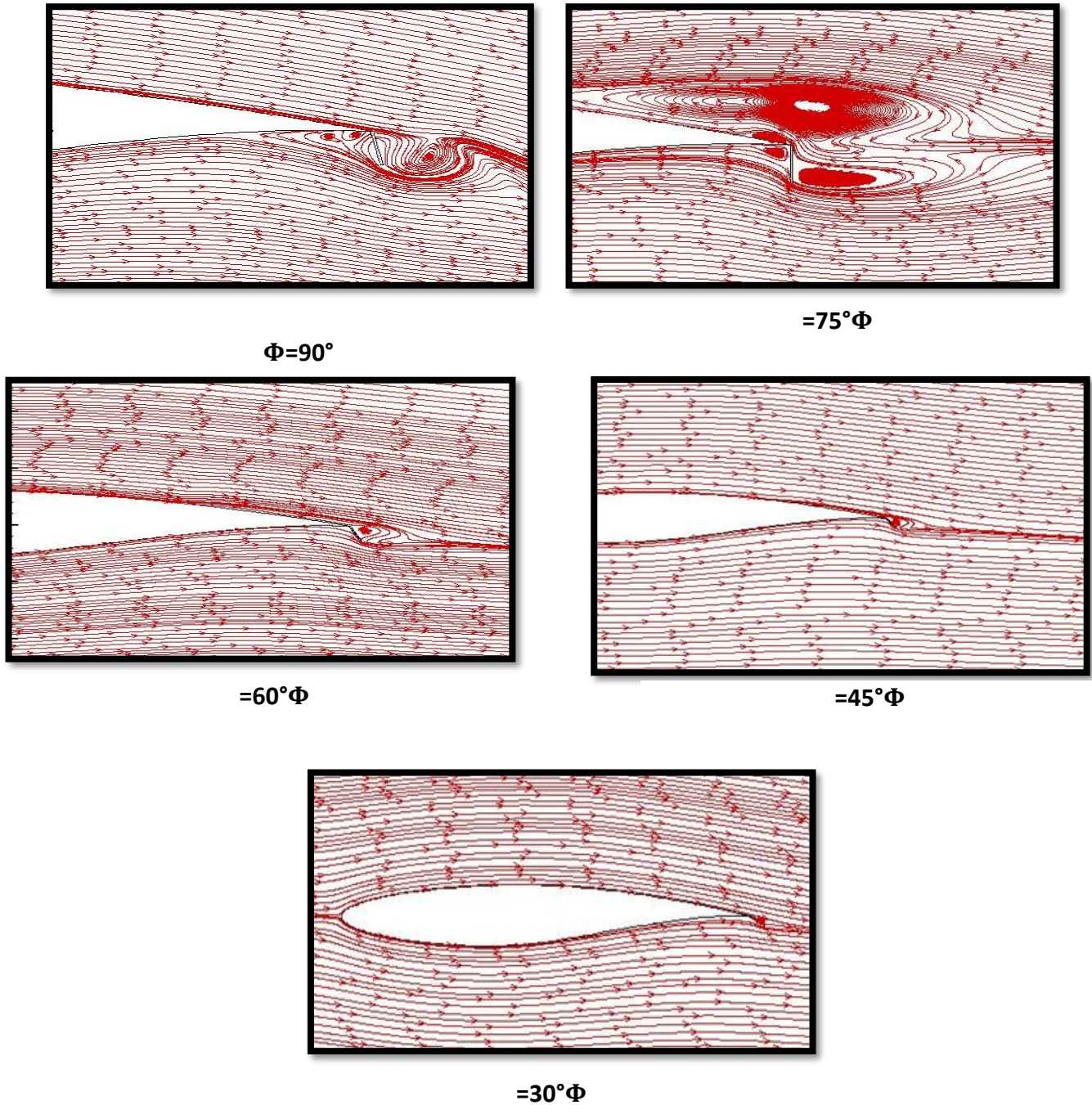


Figure 10. Streamlines for different mounting angles with 3%c height at AOA = 0°.



5.4.3 Lift coefficient

CL values for GF mounting angles of $\Phi = 30^\circ, 45^\circ, 60^\circ, 75^\circ, 90^\circ$ at $AOA=0^\circ$ have been depicted in **Fig.11**. In comparison to the airfoil without GF, the GF installation results in increasing CL by 60.88%, 66.86%, 70.48%, 67.9%, and 72.35% in the case where the GF has been mounted at $\Phi = 30^\circ, 45^\circ, 60^\circ, 75^\circ,$ and 90° , respectively. When the mounting angle ranges from 45° and 90° , the lift coefficient does not vary on a large scale. For the values of $\Phi < 45^\circ$, CL drops quite fast, thus, increasing in lift enhancement of GF, as shown in **table 4**.

Table 4. Comparison of CL values for different mounting angles of 3%c height of GF at $AOA=0^\circ$.

Φ (deg)	Computed CL	% increase in CL
Clean airfoil	0.282	
90	1.02	72.35
75	0.88	67.9
60	0.9555	70.48
45	0.851	66.86
30	0.721	60.88

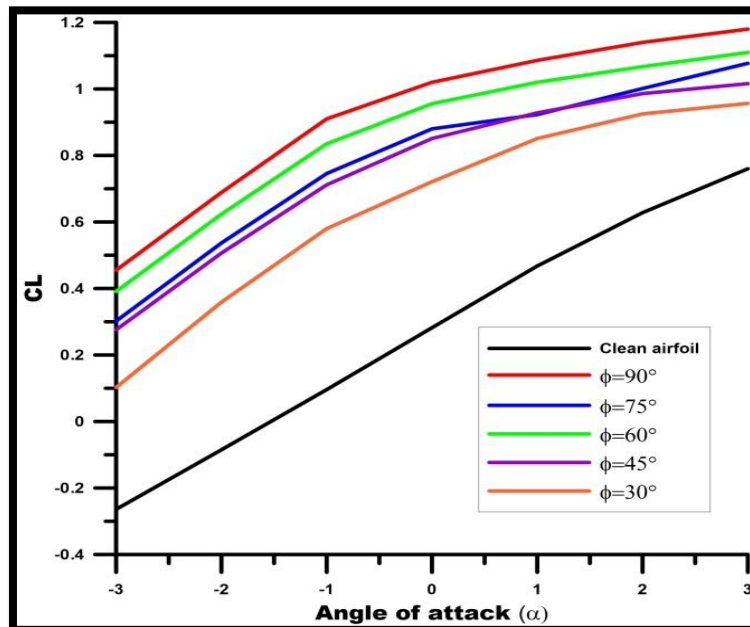


Figure 11. Variation of CL with angles of attack at different GF’s mounting angles.



5.4.4 Drag coefficient

From **Fig.12**, it can be seen that, with the increase of GF's mounting angles, the drag coefficient increases gradually for positive angles of attack but for negative angles, the CD decreases with increasing the mounting angles of GF.

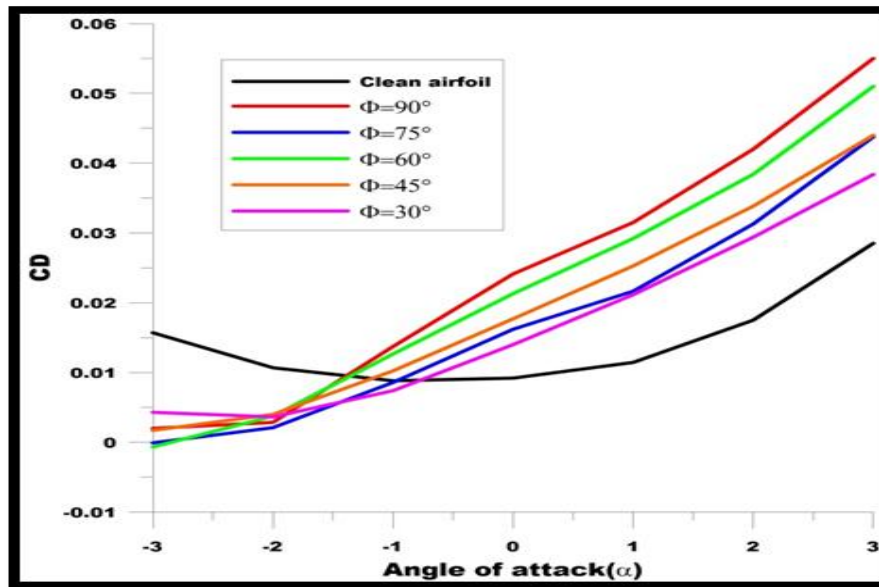


Figure 12. Variation of CD with angles of attack at different GF's mounting angles.

6. CONCLUSIONS

1. Lift enhancement is accomplished for higher GF's height values, however, at the expense of the increase in drag value. The lift increment rate decreases for larger heights, and the drag increases rapidly for $H > 2\%c$. Increasing lift coefficient as a result of altering the height of GF from $0\%c$ to $1\%c$ is more when compared to the change that has been found from the alteration of the height of GF from $2\%c$ to $3\%c$.
2. When the value of GF's height increases, the maximum suction pressure on the suction surface increases by 25.4%, 36.5%, and 68.83% when the GF height is $1\%c$, $2\%c$ and $3\%c$, respectively compared with that on the airfoil without GF.
3. The angle for zero lift decreases while the length of the gurney flap increases.
4. The shock delay results from the GF and moves downstream with increasing GF's height.
5. As the height of GF increases, the drag coefficient increases gradually for positive AOA but for negative AOA, the CD decreases with increasing the height of GF.
6. The maximum value of suction moves downstream by increasing GF's mounting angle.



7. With the decrease in GF's mounting angle, the vortex near the suction surface of the airfoil isn't entirely formed. For $\Phi < 45^\circ$, the vortex almost disappears, leading to a decrease in the suction pressure, thereby a drastic reduction in the lift coefficient.
8. When the mounting angle ranges from 45° and 90° , the lift coefficient does not vary on a large scale. For the values of $\Phi < 45^\circ$, the value of CL reduced quite rapidly.

7. NOMENCLATURE

Latin symbols

t = time

CD = Drag Coefficient

CL = Lift Coefficient

Cp = Pressure Coefficient

h = Static enthalpy, (kJ/kg)

p = Static pressure, (Pa)

q = Energy flux transferred by heat conductivity along the coordinate (x)

U = Freestream velocity, (m/s)

c = Chord length of airfoil, (m)

H = Height of Gurney flap in percentage of chord length

x = axial distance from airfoil leading edge, (m)

Greek symbols

α = Angle of attack, (deg)

ρ = Density, (kg/m³)

Φ = Mounting angle of Gurney flap with the axial chord, (deg)

τ = Shear stress, $\frac{N}{m^2}$

Abbreviations

AOA = angle of attack, (deg)

GF = Gurney flap

M = Mach number

Re = Reynolds number



8. REFERENCES

- Jang, C. S., et al., 1998. Numerical investigation of an airfoil with a Gurney flap. *Aircraft Design*, vol. 1, no. 2, pp. 75–88.
- Coakley, T. J., 1987. Numerical Simulation of Viscous Transonic Airfoil Flows. AIAA 25th Aerospace Sciences Meeting, AIAA Paper 1987- 0416.
- Cook, P. H., et al., 1979. Aerofoil RAE-2822 Pressure Distribution and Boundary Layer and Wake Measurements. AGARD Advisory Rept. 138.
- Daniel R, et al., 2006. The Effect of Gurney Flap Height on Vortex Shedding Modes Behind Symmetric Airfoils. 13th Int Symp on Applications of Laser Techniques to Fluid Mechanics, Lisbon, Portugal, 26-29 June.
- Dhruva Koti, and Ayesha Khan M., 2018. Numerical Analysis of Transonic Airfoil, *International Journal of Engineering Research & Technology (IJERT)*, Vol. 7 Issue 05.
- <http://airfoiltools.com/airfoil/naca4digit>
- Liebeck R. H., 1978. Design of Subsonic Airfoils for High Lift. *Journal of Aircraft*, Vol. 15, pp. 547-561.
- Mohammed Kheir-aldeen, and Ahmed Hamid, 2014. Experimental Study To The Effect Of Gurney Flap On The Clark Y-14 Airfoil Wing Model. *International Journal of Innovation and Scientific Research*, Vol. 9 No. 1 Sep., pp. 120-132.
- Nguyen, T.D., et al., 2019. Aerodynamic Investigations on SC-0414 Airfoil with Small High Lift Devices. *IOP Conf. Series: Journal of Physics: Conf. Series* 1215 012004.
- Nguyen, T.D., et al., 2020. Low-Speed Aerodynamic Characteristics of Supercritical Airfoil with Small High-Lift Devices from Flow Pattern Measurements. *Journal of Flow Control, Measurement & Visualization*. Vol. 8, pp. 159-172
- Xi He, et al., 2016. Numerical simulation of Gurney flap on SFYT 15 thick airfoil. *Theoretical and applied mechanics letters*, pp.286-292.